DOUBLE NEGATIVE DISPERSION RELATIONS FROM COATED PLASMONIC RODS[*]

YUE CHEN[†] AND ROBERT LIPTON[‡]

Abstract. A metamaterial with frequency dependent double negative effective properties is constructed from a subwavelength periodic array of coated rods. Explicit power series are developed for the dispersion relation and associated Bloch wave solutions. The expansion parameter is the ratio of the length scale of the periodic lattice to the wavelength. Direct numerical simulations for finite size period cells show that the leading order term in the power series for the dispersion relation is a good predictor of the dispersive behavior of the metamaterial.

1. Introduction. Metamaterials are artificial materials designed to have electromagnetic properties not generally found in nature. One contemporary area of research explores novel subwavelength constructions that deliver metamaterials with both a negative bulk dielectric constant and bulk magnetic permeability across certain frequency intervals. These double negative materials are promising materials for the creation of negative index superlenses that overcome the small diffraction limit and have great potential in applications such as biomedical imaging, optical lithography, and data storage. The early work of Veselago [39] identified novel effects associated with hypothetical materials for which both the dielectric constant and magnetic permeability are simultaneously negative. Such double negative media support electromagnetic wave propagation in which the phase velocity is antiparallel to the direction of energy flow and other unusual electromagnetic effects, such as the reversal of the Doppler effect and Cerenkov radiation. At the end of the last century Pendry et al. [26] demonstrated that unconventional properties can be derived from subwavelength configurations of different conventional materials and showed that a cubic lattice of metal wires exhibits behavior associated with a negative bulk dielectric constant. Subsequently it was shown that a periodic array of nonmagnetic metallic split-ring resonators delivers negative effective magnetic permeability at microwave frequencies [27]. In a more recent work Smith et al. [36] experimentally demonstrated that metamaterials made from arrays of metallic posts and split-ring resonators generate an effective negative refractive index at microwave frequencies. Building on this Shelby, Smith, and Schultz [33] experimentally confirmed that a microwave beam would undergo negative refraction at the interface between such a metamaterial and air. Subsequent work has delivered several new designs using different configurations of metallic resonators for double negative behavior [14, 19, 32, 44, 45, 48].

For higher frequencies in the infrared and optical ranges, new strategies for gen-

[†]Department of Mathematics, University of Kentucky, Lexington, KY 40506 (chenyue0715@uky.edu).

[‡]Department of Mathematics, Louisiana State University, Baton Rouge, LA 70803 (lipton@math.lsu.edu).

erating materials with double negative bulk properties rely on Mie resonances. One scheme employs coated rods made from a high dielectric core coated with a frequency dependent dielectric plasmonic or Drude-type behavior at optical frequencies [41, 42, 43]. A second scheme employs small rods or particles made from dielectric materials with large permittivity [18, 28, 40]. Alternate strategies for generating negative bulk dielectric permeability at infrared and optical frequencies use special configurations of plasmonic nanoparticles [2, 35]. The list of metamaterial systems is rapidly growing, and comprehensive reviews of the subject can be found in [30, 31].
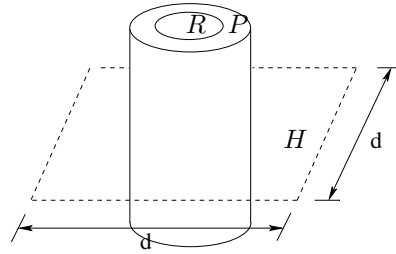

FIG. 1. *Coated cylinder microgeometry: R represents the high dielectric core and P the plasmonic coating, and H denotes the connected host material.*

In this article we construct metamaterials made from subwavelength periodic arrangements of nonmagnetic infinitely long coated cylinders immersed in a nonmagnetic host. The coated cylinders are parallel to the x_3 axis and made from a frequency independent high dielectric core and a frequency dependent dielectric plasmonic coating (Figure 1). For this case we are able to express the effective dielectric constant and magnetic permeability in terms of spectral representation formulas. These formulas are determined by the Dirichlet spectra of the core and the generalized electrostatic resonances associated with the region exterior to the core. The formulas are used to calculate the frequency intervals where either double negative or double positive bulk properties appear. These intervals are governed by the poles and zeros of the effective magnetic permeability and effective dielectric permittivity tensors.

These formulas are not found by effective medium approximations such as those based on the Clausius–Mossotti formula, but instead they appear as leading order terms of an explicit multiscale expansion for the solution of Maxwell's equations. The expansion parameter is the period of the crystal "d." Denoting the wavelength by λ and wave number by $k = 2\pi/\lambda$ we investigate wave propagation in the subwavelength regime $\eta = dk < 1$. Explicit power series are developed in η for the dispersion relation and associated Bloch wave solutions. It is shown that the frequency intervals over which the effective properties are either double negative or double positive imply the existence of convergent power series representations for Bloch wave modes in the dynamic regime away from the homogenization limit $\eta \to 0$. We apply the power series representation to calculate the average Poynting vector and show that in the homogenization limit the energy flow and phase velocity are in opposite directions over frequency intervals associated with double negative behavior. This gives the requisite explicit and mathematically rigorous analysis beyond the homogenization limit and provides evidence for wave propagation in the double negative regime for this class of metamaterial.

To fix ideas we assume that the host medium containing the coated rods has relative dielectric permittivity equal to unity. In order to generate effective magnetic

properties our strategy is to follow Bouchitté and Felbacq [7] and suppose that the material comprising the core phase of the rod is a high contrast dielectric material $\epsilon_R = \gamma d^2$. This scaling of the material coefficients is seen in homogenization of double porosity models [47] and high contrast dielectric media [46, 3].

In order to generate negative effective dielectric permittivity we recall the notion of electrostatic resonances [4, 21, 23]. Here we introduce a new type of electrostatic resonance for a high contrast three phase medium. These resonances depend only on the geometry; see (2.14) and (2.15). To excite the resonances and drive the effective dielectric constant negative we choose a frequency dependent dielectric coating. In this paper the coating has the dielectric constant given by the Drude model [41, 42]

$$(1.1) \qquad \epsilon_P(\omega^2) = 1 - \frac{\omega_p^2}{\omega^2},$$

where ω is the frequency and ω_p is the plasma frequency [5].

Homogenization methods for spectral problems involving two phase high contrast mixtures have been developed based on strong two scale resolvent convergence [47, 46]. The associated corrector theory is developed in [3]. In this paper we address a spectral problem for three phase media which in addition to a high contrast phase has a third phase with a dielectric constant that can be large and negative. This feature renders the associated two scale operator noncoercive. The approach taken here differs from the two scale approach and represents solutions as convergent power series in η. The power series approach to subwavelength analysis has been developed and utilized in [16] to characterize the dynamic dispersion relations for Bloch waves inside plasmonic crystals. It has also been extended and applied to assess the influence of effective negative permeability on the propagation of Bloch waves inside high contrast dielectrics [17], for the generation of negative permeability inside metallic-dielectric resonators [34], and for concentric coated cylinder assemblages generating a double negative media [11]. Earlier work introduces convergent power series for two phase high contrast media in the electrostatic case [10].

For the problem treated here the series is shown to be absolutely summable in the H^1 norm inside frequency intervals that do not intersect the Dirichlet and electrostatic spectra [12]. One advantage of the power series approach is that it does not require the coercivity of the two scale operator. The power series provides an approximation of the solution in the H^1 norm up to any algebraic order in η. The series are presented in section 2 and are easily seen to be strongly two scale convergent in the $\eta \to 0$ limit.

We apply the methods to a metamaterial made from a periodic array of circular coated cylinders making use of the method of Rayleigh (see [38]) to numerically calculate the generalized electrostatic resonances. These resonances together with the Dirichlet spectra of the core are used to identify explicit frequency intervals over which effective properties are double negative or double positive. Several branches of the leading order dispersion relation are calculated using the spectral representation formulas for the effective magnetic permeability and dielectric constant. We compare these with direct numerical simulations to find that the leading order dispersion relation is a good predictor of the dispersive behavior of the metamaterial. It is found that the leading order behavior trends with the direct numerical simulation even when the length scale of the microstructure is only 20% smaller than the wavelength of the propagating wave. These results provide new methods necessary to identify frequency intervals characterized by negative index behavior and its influence on wave propagation beyond the homogenization limit.

Related work delivers formulas for frequency dependent effective magnetic permeability together with conditions for the generation of negative effective permeability [9, 8, 7, 13, 15, 20]. For periodic arrays made from metal fibers a homogenization theory delivering a negative effective dielectric constant [6] has been established. A novel method for creating metamaterials with prescribed effective dielectric permittivity and effective magnetic permeability at a fixed frequency is developed in [24]. New methodologies for computing homogenized properties for metamaterials are presented in [1, 37].
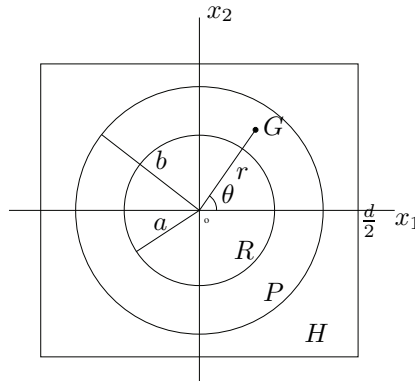

FIG. 2. *The period cell.*

2. Power series representations. We start with a metamaterial crystal characterized by a period cell containing a centered coated cylinder with a plasmonic coating and a high dielectric core. The core radius and the coating radius are denoted by a and b, respectively (Figure 2). The cylinder is parallel to the x_3 axis and is periodically arranged within a square lattice over the transverse $\mathbf{x} = (x_1, x_2)$ plane. The period of the lattice is denoted by d. For H-polarized Bloch waves, the magnetic field is aligned with the cylinders and the electric field lies in the transverse plane. The direction of propagation is described by the unit vector $\hat{\kappa} = (\kappa_1, \kappa_2)$, $k = 2\pi/\lambda$ is the wave number for a wave of length λ, and the fields are of the form

$$(2.1) \quad H_3 = H_3(\mathbf{x})e^{i(k\hat{\kappa}\cdot\mathbf{x}-t\omega)}, \quad E_1 = E_1(\mathbf{x})e^{i(k\hat{\kappa}\cdot\mathbf{x}-t\omega)}, \quad E_2 = E_2(\mathbf{x})e^{i(k\hat{\kappa}\cdot\mathbf{x}-t\omega)},$$

where $H_3(\mathbf{x})$, $E_1(\mathbf{x})$, and $E_2(\mathbf{x})$ are d-periodic for $\mathbf{x}$ in $\mathbb{R}^2$. Here c denotes the speed of light in free space. We denote the unit vector pointing along the x_3 direction by $\mathbf{e}_3$, and the periodic dielectric permittivity and magnetic permeability are denoted by a_d and μ, respectively. The electric field component $\mathbf{E} = (E_1, E_2)$ of the wave is determined by

$$(2.2) \qquad \mathbf{E} = -\frac{ic}{\omega a_d}\mathbf{e}_3 \times \nabla H_3.$$

The materials are assumed nonmagnetic, and hence the magnetic permeability μ is set to unity inside the coated cylinder and host. The oscillating dielectric permittivity for the crystal is a d periodic function in the transverse plane and is described by $a_d = a_d(\mathbf{x}/d)$, where $a_d(\mathbf{y})$ is the unit periodic dielectric function taking the values

$$(2.3) \quad a_d(\mathbf{y}) = \begin{cases} \epsilon_H & \text{in the host material,} \\ \epsilon_P(\omega) & \text{in the frequency dependent "plasmonic" coating,} \\ \epsilon_R = \gamma/d^2 & \text{in the high dielectric core.} \end{cases}$$

Here γ has dimensions of area and the frequency dependent permittivity ϵ_P of the plasmonic coating is given by (1.1), where ω is the frequency and ω_p is the plasma frequency [5]. Setting $h^d(\mathbf{x}) = H_3(\mathbf{x})e^{i(k\hat{\kappa}\cdot\mathbf{x})}$ the Maxwell equations take the form of the Helmholtz equation given by

$$(2.4) \qquad -\nabla_{\mathbf{x}} \cdot \left(a_d^{-1}\left(\frac{\mathbf{x}}{d}\right)\nabla_{\mathbf{x}}h^d(\mathbf{x})\right) = \frac{\omega^2}{c^2}h^d \quad \text{in } \mathbb{R}^2.$$

We set $\mathbf{x} = d\mathbf{y}$ for $\mathbf{y}$ inside the unit period $Y = [-0.5, 0.5]^2$, put $\beta = dk\hat{\kappa}$, and write $u(\mathbf{y}) = H_3(d\mathbf{y})$. The dependent variable is written as $u^d(\mathbf{y}) = h^d(d\mathbf{y}) = u(\mathbf{y})\exp^{i\beta\cdot\mathbf{y}}$, and we recover the equivalent problem over the unit period cell given by

$$(2.5) \qquad -\nabla_{\mathbf{y}} \cdot \left(a_d^{-1}(\mathbf{y})\nabla_{\mathbf{y}}u^d\right) = \frac{d^2\omega^2}{c^2}u^d \quad \text{in } Y.$$

We start by introducing the power series in terms of dimensionless groups given by the ratio $\rho = d/\sqrt{\gamma}$, wave number $\tau = \sqrt{\gamma}k$, and square frequency $\xi = \gamma\frac{\omega^2}{c^2}$. The dimensionless parameter measuring the departure away from quasi-static or homogenization limits is given by the ratio of period size to wavelength $\eta = dk = \rho\tau \geq 0$. For the problem considered here the $d = 0$ limit is distinct from the quasi-static limit $k = 0$. This is due to the explicit dependence of the dielectric constant on d inside the core region of the rod.

In these new dimensionless parameters the dielectric permittivity is given by $\epsilon_P = 1 - \frac{\gamma\omega_p^2/c^2}{\xi}$, $\epsilon_R = \frac{1}{\rho^2}$, $\epsilon_H = 1$. The associated piecewise constant dielectric permittivity is denoted by $a_\rho(\mathbf{y})$ for $\mathbf{y}$ in Y with

$$(2.6) \qquad a_\rho(\mathbf{y}) = \begin{cases} \epsilon_H = 1 & \text{in the host material,} \\ \epsilon_P = 1 - \frac{\gamma\omega_p^2/c^2}{\xi} & \text{in the "plasmonic" coating,} \\ \epsilon_R = \frac{1}{\rho^2} & \text{in the high dielectric core,} \end{cases}$$

and (2.5) is given by

$$(2.7) \qquad -\nabla_{\mathbf{y}} \cdot \left(a_\rho^{-1}(\mathbf{y})\nabla_{\mathbf{y}}u^d(\mathbf{y})\right) = \rho^2\xi u^d(\mathbf{y}) \quad \text{in } Y.$$

The small parameter for this problem is ρ, and in what follows we develop power series in the parameter $\eta = \rho\tau$. We introduce the space $H_{per}^1(Y)$ of trial and test functions that are square integrable with periodic boundary conditions on Y and square integrable derivatives. The equivalent variational form of (2.7) is given by

$$(2.8) \qquad \int_Y a_\rho^{-1}\nabla u^d \cdot \nabla\bar{\tilde{v}} = \int_Y \frac{\rho^2\xi}{c^2}u^d\bar{\tilde{v}}$$

for any $\tilde{v} = v(\mathbf{y})e^{i\hat{\kappa}\cdot\tau\rho\mathbf{y}}$, where $v \in H_{per}^1(Y)$. On substitution of $u^d = u(\mathbf{y})e^{i\hat{\kappa}\cdot\tau\rho\mathbf{y}}$ and $\tilde{v} = v(\mathbf{y})e^{i\hat{\kappa}\cdot\tau\rho\mathbf{y}}$ we transform (2.8) into

$$\int_H \tau^2\left(\xi - \gamma\frac{\omega_p^2}{c^2}\right)(\nabla + i\eta\hat{\kappa})u \cdot \overline{(\nabla + i\eta\hat{\kappa})v} + \int_P \tau^2\xi(\nabla + i\eta\hat{\kappa})u \cdot \overline{(\nabla + i\eta\hat{\kappa})v}$$

$$+ \int_R \eta^2\left(\xi - \gamma\frac{\omega_p^2}{c^2}\right)(\nabla + i\eta\hat{\kappa})u \cdot \overline{(\nabla + i\eta\hat{\kappa})v} = \int_Y \eta^2\xi\left(\xi - \gamma\frac{\omega_p^2}{c^2}\right)u\overline{v}.$$

(2.9)

The unit period cell for the generic metamaterial system is represented in Figure 2. In what follows, R represents the rod core cross section containing high dielectric material and P the coating containing the plasmonic material, and H denotes the connected host material. Following [12] we introduce the expansions for the pair u, ξ

$$(2.10) \qquad u = \sum_{m=0}^{\infty} \eta^m u_m,$$

$$(2.11) \qquad \xi = \sum_{m=0}^{\infty} \eta^m \xi_m,$$

where u_m belong to $H_{per}^1(Y)$. In view of the algebra it is convenient to write $u_m = i^m \underline{u}_0 \psi_m$, where $\underline{u}_0$ is an arbitrary constant factor. Substitution of (2.10) and (2.11) into (2.9) and equating like powers of η delivers an infinite coupled system of equations that can be solved iteratively. We now describe this system of equations expressed in variational form. Set

$$z = \epsilon_P^{-1}(\xi_0) = \left(1 - \frac{\gamma \omega_p^2/c^2}{\xi_0}\right)^{-1},$$

and for u, v belonging to $H_{per}^1(Y)$ we introduce the sesquilinear form

$$(2.12) \qquad B_z(u,v) = \int_H \nabla u \cdot \nabla \overline{v}\, d\mathbf{y} + \int_P z\, \nabla u \cdot \nabla \overline{v}\, d\mathbf{y}.$$

Here $Y \setminus R = H \cup P$. Substitution of the series into (2.9) and equating like powers of η produces the infinite set of coupled equations for $m = 0, 1, 2 \ldots$ given by

$$\tau^2 B_z(\psi_m, v)$$

$$+ \xi_0^{-1} \epsilon_p^{-1}(\xi_0) \tau^2 \int_{Y \setminus R} \left[\sum_{l=1}^{m-1} (-i)^l \xi_l \nabla \psi_{m-l} \cdot \nabla \overline{v} \right.$$

$$+ \hat{\kappa} \cdot \sum_{l=0}^{m-1} (-i)^l \xi_l (\psi_{m-1-l} \nabla \overline{v} - \nabla \psi_{m-1-l} \overline{v}) - \sum_{l=0}^{m-2} (-i)^l \xi_l \psi_{m-2-l} \overline{v} \Bigg]$$

$$- \xi_0^{-1} \epsilon_p^{-1}(\xi_0) \tau^2 \gamma \frac{\omega_p^2}{c^2} \int_H \left[\hat{\kappa} \cdot (\psi_{m-1} \nabla \overline{v} - \nabla \psi_{m-1} \overline{v}) - \psi_{m-2} \overline{v} \right]$$

$$- \xi_0^{-1} \epsilon_p^{-1}(\xi_0) \int_R \left[\sum_{l=0}^{m-2} (-i)^l \xi_l \nabla \psi_{m-2-l} \cdot \nabla \overline{v} + \hat{\kappa} \cdot \sum_{l=0}^{m-3} (-i)^l \xi_l (\psi_{m-3-l} \nabla \overline{v} \right.$$

$$- \nabla \psi_{m-3-l} \overline{v}) - \sum_{l=0}^{m-4} (-i)^l \xi_l \psi_{m-4-l} \overline{v} \Bigg]$$

$$+ \xi_0^{-1} \epsilon_p^{-1}(\xi_0) \int_R \gamma \frac{\omega_p^2}{c^2} \left[\nabla \psi_{m-2} \cdot \nabla \overline{v} + \psi_{m-4} \overline{v} + \hat{\kappa} \cdot (\psi_{m-3} \nabla \overline{v} - \nabla \psi_{m-3} \overline{v}) \right]$$

$$- \xi_0^{-1} \epsilon_p^{-1}(\xi_0) \int_Y \left[\sum_{l=0}^{m-2} \sum_{n=0}^{l} \xi_{m-2-l} \xi_n \psi_{l-n} i^{l-n-m} \overline{v} \right.$$

$$+ \gamma \frac{\omega_p^2}{c^2} \sum_{l=0}^{m-2} (-i)^l \xi_l \psi_{m-2-l} \overline{v} \Bigg] = 0 \quad \text{for all } v \text{ in } H_{per}^1(Y).$$

$$(2.13)$$

Here the convention is $\psi_m = 0$ for $m < 0$.

The determination of the elements belonging to $\{\psi_m\}_{m=0}^{\infty}$ proceeds iteratively. One starts by determining ψ_0 on $Y \setminus R$; this function is used as boundary data to determine ψ_0 in R, from which we determine ψ_1 on $Y \setminus R$, and the full sequence is determined on iterating this cycle. The elements ξ_m are recovered from solvability conditions obtained by setting $v = 1$ in (2.13) and proceeding iteratively.

Applying the theory developed in [12] the solvability of the infinite system for determining the unknown functions $\{\psi_m\}_{m=1}^{\infty}$ depends on the Dirichlet spectra of R and the generalized electrostatic spectra associated with $Y \setminus R = P \cup H$. Here the Dirichlet spectra are given by the eigenvalues $\nu_n > 0$, $\nu_{n+1} \geq \nu_n$, $\nu_n \to \infty$ for $n \to \infty$ associated with the Dirichlet eigenfunctions of the Laplacian on R. The generalized electrostatic spectra are characterized by all eigenvalues λ and eigenfunctions u of

$$(2.14) \qquad \begin{cases} \Delta u = 0 & \text{in } H, \\ \Delta u = 0 & \text{in } P, \end{cases}$$

with the boundary conditions

$$(2.15) \qquad \begin{cases} u|^{-} = u|^{+} & \text{on } \partial P, \\ \partial_r u|_{r=a} = 0 & \text{on } \partial R, \\ \lambda[\partial_r u]_{+}^{-} = -\frac{1}{2}(\partial_r u^{-} + \partial_r u^{+}) & \text{on } \partial P, \\ u \text{ is } Y\text{-periodic.} \end{cases}$$

The generalized electrostatic spectra being denumerable lies in the open interval $(-\frac{1}{2}, \frac{1}{2})$ with zero being the only accumulation point; see [12]. The eigenfunctions $\{\psi_{\lambda_n}\}_{n=0}^{\infty}$ associated with the electrostatic resonances $\{\lambda_n\}_{n=1}^{\infty}$ form a complete orthonormal set of functions in the space of mean zero periodic functions belonging to $H_{per}^1(Y \setminus R)$ that are harmonic in P and H [12]. Here orthonormality is with respect to the inner product $(u, v) = \int_{Y \setminus R} \nabla u \cdot \nabla \overline{v} \, dx$. The complete orthonormal systems of eigenfunctions associated with electrostatic resonances and Dirichlet eigenvalues are used to solve for ψ_0 and ψ_1 in $H \cup P$ and provide an explicit formula for ξ_0.

We now follow [12] and identify the first two terms of the power series ψ_0 and ψ_1 to recover the dispersion relation for the leading order term $\omega^2/c^2 = \gamma^{-1}\xi_0$. From (2.13) we read that ψ_0 is the solution of

$$(2.16) \qquad B_z(\psi_0, v) = 0 \quad \text{for all } v \text{ in } H^1(Y \setminus R).$$

Next observe that a straightforward calculation gives the following dichotomy:
1. $\xi_0 = \zeta_n = (\lambda_n + 1/2)\gamma\omega_p^2/c^2$, $n = 1, \ldots$, and ψ_0 is an eigenfunction for (2.14), (2.15).
2. $\xi_0 \neq \zeta_n = (\lambda_n + 1/2)\gamma\omega_p^2/c^2$, $n = 1, \ldots$, and $\psi_0 = \text{const}$.

Here we choose the second alternative. Subsequent work will investigate the case when the first alternative is applied. Restricting ourselves to test functions v with support in R in (2.13) we get

$$(2.17) \qquad \int_R (\nabla \psi_0 \cdot \nabla \overline{v} - \xi_0 \psi_0 \overline{v}) \, d\mathbf{y} = 0.$$

From continuity we have the boundary condition for ψ_0 on R given by $\psi_0 = \text{const}$. Here we have the following alternatives:
1. If ξ_0 is a Dirichlet eigenvalue ν_i of $-\Delta$ in R, then $\psi_0(\mathbf{y}) = 0$ for $\mathbf{y}$ in $Y \setminus R$.

2. If $\xi_0 \neq \nu_i$, $i = 1, 2, \ldots$, then ψ_0 is the unique solution of the Helmholtz equation (2.17) and $\psi_0 = \text{const}$ in $Y \setminus R$.

In this treatment we will choose the second alternative $\xi_0 \neq \nu_i$. The case when the first alternative is chosen will be taken up in future investigation. Since $u_0 = \underline{u}_0 \psi_0$, where $\underline{u}_0$ is an arbitrary constant, we can without loss of generality make the choice $\psi_0 = 1$ for $\mathbf{y}$ in $Y \setminus R$. Since $\xi_0 \neq \nu_i$, $i = 1, \ldots$, and $\psi_0 = 1$ in $Y \setminus R$, a straightforward calculation gives ψ_0 in R in terms of the complete set of Dirichlet eigenfunctions and eigenvalues:

$$(2.18) \qquad \psi_0 = \sum_{n=1}^{\infty} \frac{\mu_n \langle \phi_n \rangle_R}{\mu_n - \xi_0} \phi_n = 1 + \xi_0 \sum_{n=1}^{\infty} \frac{\langle \phi_n \rangle_R}{\mu_n - \xi_0} \phi_n \quad \text{in } R.$$

Note here that μ_n denote the Dirichlet eigenvalues of $-\Delta$ in R whose eigenfunctions ϕ_n have nonzero mean, $\langle \phi_n \rangle_R = \int_R \phi_n(y) dy \neq 0$.

To find ψ_1 in $Y \setminus R$, we appeal to (2.13) with $\psi_0 = 1$ in $Y \setminus R$ to discover

$$(2.19) \qquad B_z(\psi_1, v) = -\int_H \hat{\kappa} \cdot \nabla \overline{v} - \int_P \epsilon_P^{-1}(\xi_0) \hat{\kappa} \cdot \nabla \overline{v} \quad \text{for all } v \in H_{per}^1(Y).$$

The problem has a unique solution subject to the mean-zero condition $\int_{Y \setminus R} \psi_1 = 0$, provided that $\xi_0 \neq \zeta_i$, $i = 1, 2, \ldots$. We represent ψ_1 in terms of the complete set of orthonormal eigenfunctions $\{\psi_{\lambda_n}\}_{n=1}^{\infty}$ associated with the generalized electrostatic resonances $\{\lambda_n\}_{n=1}^{\infty}$. Expanding ψ_1 in terms of the complete set of orthonormal eigenfunctions $\{\psi_{\lambda_n}\}$ we obtain the representation

$$(2.20) \qquad \psi_1 = - \sum_{-\frac{1}{2} < \lambda_n < \frac{1}{2}} \left(\frac{(\alpha_{\lambda_n}^1 + \epsilon_P^{-1}(\xi_0) \alpha_{\lambda_n}^2)}{1 + (\epsilon_P^{-1}(\xi_0) - 1)(1 - \lambda_n)} \right) \psi_{\lambda_n} \quad \text{in } Y \setminus R$$

with

$$(2.21) \qquad \alpha_{\lambda_n}^1 = \hat{\kappa} \cdot \int_H \nabla \psi_{\lambda_n} \, d\mathbf{y} \quad \text{and} \quad \alpha_{\lambda_n}^2 = \hat{\kappa} \cdot \int_P \nabla \psi_{\lambda_n} \, d\mathbf{y}.$$

Setting $v = 1$ and $m = 2$ in (2.13) we recover the solvability condition given by

$$(2.22) \qquad \tau^2 \int_{H \cup P} \left[-\hat{\kappa} \cdot \xi_0 \nabla \psi_1 + \xi_0 \right] - \tau^2 \gamma \frac{\omega_p^2}{c^2} \int_H (-\hat{\kappa} \nabla \psi_1 + 1)$$
$$= \int_Y \left(\xi_0^2 \psi_0 - \gamma \frac{\omega_p^2}{c^2} \xi_0 \psi_0 \right).$$

Substitution of the spectral representations for ψ_1 and ψ_0 given by (2.20) and (2.18) into (2.22) delivers the homogenized dispersion relation

$$(2.23) \qquad \xi_0 = \tau^2 n_{eff}^{-2}(\xi_0),$$

where the effective index of diffraction n_{eff}^2 depends upon the direction of propagation $\hat{\kappa}$ and is written as

$$(2.24) \qquad n_{eff}^2(\xi_0) = \frac{\mu_{eff}(\xi_0)}{\epsilon_{eff}^{-1}(\xi_0) \hat{\kappa} \cdot \hat{\kappa}}.$$

The frequency dependent effective magnetic permeability μ_{eff} and effective dielectric permittivity ϵ_{eff} are given by

$$(2.25) \qquad \mu_{eff}(\xi_0) = \int_Y \psi_0 = \theta_H + \theta_P + \sum_{n=1}^{\infty} \frac{\mu_n \langle \phi_n \rangle_R^2}{\mu_n - \xi_0}$$

and

$$\epsilon_{eff}^{-1}(\xi_0)\hat{\kappa} \cdot \hat{\kappa} = \int_{Y \backslash R} a_d^{-1}(y)(\nabla\psi_1 + \hat{\kappa}) \cdot \hat{\kappa} \, dy = \int_{Y \backslash R} a_d^{-1}(y)(\nabla\psi_1 + \hat{\kappa}) \cdot \overline{(\nabla\psi_1 + \hat{\kappa})} \, dy$$

$$(2.26) \qquad = \theta_H + \frac{\xi_0}{\xi_0 - \frac{\gamma\omega_p^2}{c^2}}\theta_P$$

$$- \sum_{-\frac{1}{2} < \lambda_h < \frac{1}{2}} \left(\frac{\left(\xi_0 - \frac{\gamma\omega_p^2}{c^2}\right)|\alpha_{\lambda_h}^{(1)}|^2 + 2\frac{\gamma\omega_p^2}{c^2}\alpha_{\lambda_h}^{(1)}\alpha_{\lambda_h}^{(2)} + \frac{\left(\frac{\gamma\omega_p^2}{c^2}\right)^2}{\xi_0 - \frac{\gamma\omega_p^2}{c^2}}|\alpha_{\lambda_h}^{(2)}|^2}{\xi_0 - (\lambda_h + \frac{1}{2})\frac{\gamma\omega_p^2}{c^2}} \right),$$

where θ_H and θ_P are the areas occupied by regions H and P, respectively.

Writing the dispersion relation (2.23) explicitly in terms of μ_{eff} and ϵ_{eff} gives

$$(2.27) \qquad \mu_{eff}(\xi_0)\xi_0 = \tau^2\epsilon_{eff}^{-1}(\xi_0)\hat{\kappa} \cdot \hat{\kappa}.$$

From (2.27) it is evident that there is a solution ξ_0 over intervals for which $\mu_{eff}(\xi_0)$ and $\epsilon_{eff}^{-1}(\xi_0)\hat{\kappa}\cdot\hat{\kappa}$ have the same sign. It is also clear that there are an infinite number of intervals of the dispersion relation for which this is true, and the branches of solutions to (2.27) are labeled $\{\xi_0^n\}_{n=1}^{\infty}$. We explicitly note the dependence of these branches on the wave number τ and propagation direction $\hat{\kappa}$ and write $\xi_0^n(\tau, \hat{\kappa})$. The power series for each branch of the dispersion relation and the associated transverse magnetic Bloch wave solution of (2.4) are given by

$$(2.28) \qquad \xi^n = \xi_0^n(\tau, \hat{\kappa}) + \sum_{l=1}^{\infty}(\tau\rho)^l \xi_l^n$$

for

$$(2.29) \qquad \{-2\pi \leq \tau\rho\hat{\kappa}_1 \leq 2\pi, -2\pi \leq \tau\rho\hat{\kappa}_2 \leq 2\pi\},$$

and

$$(2.30) \qquad H_3^n = \underline{u}_0\left(\psi_0^n(\mathbf{x}/d) + \sum_{l=1}^{\infty}(\tau\rho)^l i^l \psi_l^n(\mathbf{x}/d)\right)\exp\left\{i\left(k\hat{\kappa}\cdot\mathbf{x} - t\omega\right)\right\},$$

where

$$(2.31) \qquad \frac{\omega}{c} = \sqrt{\frac{\xi^n}{\gamma}}.$$

For each branch of the dispersion relation, the series (2.30) is absolutely summable in $H^1(Y)$ and (2.31) converges for ρ sufficiently small; this follows from the theory developed in [12].

The power series for the solution and dispersion relation provide a complete description of the waves inside metamaterials for ρ sufficiently small. These expansions can be used to identify homogenization limits. The strong two scale limit can be read directly from the power series. For any branch of the dispersion relation the Bloch wave factor appearing in (2.30) is written as

$$(2.32) \qquad H_\rho(\mathbf{x}) = \underline{u}_0 \left(\psi_0(\mathbf{x}/d) + \sum_{l=1}^{\infty} (\rho\tau)^l i^l \psi_l(\mathbf{x}/d) \right) e^{i(k\hat{\kappa}\cdot\mathbf{x})}.$$

The absolute summability of the series immediately implies the strong two scale convergence of $H_\rho(\mathbf{x})$ to the two scale limit $H_0(\mathbf{x},\mathbf{y})$ as $\rho \to 0$ given by

$$(2.33) \qquad H_0(\mathbf{x},\mathbf{y}) = \underline{u}_0 \psi_0(\mathbf{y}) e^{i(k\hat{\kappa}\cdot\mathbf{x})},$$

$$(2.34) \qquad \mu_{eff}(\gamma\omega^2/c^2)\gamma\omega^2/c^2 = k^2 \epsilon_{eff}^{-1}(\gamma\omega^2/c^2)\hat{\kappa}\cdot\hat{\kappa}.$$

The homogenization limit is obtained on integrating (2.33) over the unit period cell. The homogenized wave is a plane wave for the dispersive magnetic "effective medium" with

$$(2.35) \qquad B_{hom}(\mathbf{x}) = \int_Y H_0(\mathbf{x},\mathbf{y})\,d\mathbf{y} = \underline{u}_0 \mu_{eff}(\gamma\omega^2/c^2) e^{i(k\hat{\kappa}\cdot\mathbf{x})},$$

where k and ω satisfy (2.34).

In the limit $\omega_p = 0$, the coating and host have the same dielectric constant and the dispersion relation (2.34) naturally recovers the continuous spectrum for the two scale limit of the double porosity model treated in [47, 46, 3]; see also [17].

3. Homogenization and energy flow for double negative effective properties. The power series representation is used to show that branches of solutions (2.27) corresponding to $\mu_{eff}(\xi_0) < 0$, $\epsilon_{eff}^{-1}(\xi_0)\hat{\kappa}\cdot\hat{\kappa} < 0$ correspond to frequency intervals where the phase velocity in the effective medium is opposite to the direction of energy flow. For H-polarized Bloch waves, the magnetic field $\mathbf{H}(\mathbf{x}/d) = (0,0,H_3(\mathbf{x}/d))$, where $H_3(\mathbf{x}/d)$ is given by (2.30), and the electric field $\mathbf{E}(\mathbf{x}/d) = (E_1(\mathbf{x}/d), E_2(\mathbf{x}/d), 0)$. Both fields are related through (2.2). Therefore

$$(3.1) \qquad \mathbf{E}(\mathbf{x}/d) = \frac{ic}{\omega a_d}\partial_{x_2}H_3(\mathbf{x}/d)\mathbf{e_1} - \frac{ic}{\omega a_d}\partial_{x_1}H_3(\mathbf{x}/d)\mathbf{e_2},$$

where $\mathbf{e_i}$ is the unit vector along the x_i direction for $i = 1,2,3$. The time average of the Poynting vector is given by

$$(3.2) \qquad \begin{aligned} \mathbf{P}^d &= \frac{1}{2}Re[\mathbf{E}(\mathbf{x}/d) \times \overline{\mathbf{H}(\mathbf{x}/d)}] \\ &= \frac{1}{2}Re[E_2(\mathbf{x}/d)\overline{H_3(\mathbf{x}/d)}\mathbf{e_1} - E_1(\mathbf{x}/d)H_3(\mathbf{x}/d)\mathbf{e_2}]. \end{aligned}$$

Consider any fixed averaging domain D transverse to the cylinders, and the spatial average of the electromagnetic energy flow along the direction $\hat{\kappa}$ over this domain is written as $\langle \mathbf{P}^d \cdot \hat{\kappa}\rangle_D$. Substituting (2.30) and (3.1) into (3.2), a straightforward calculation shows that the average electromagnetic energy flow along the direction $\hat{\kappa}$ in the homogenization limit is given by

$$(3.3) \qquad \lim_{d\to 0}\langle \mathbf{P}^d \cdot \hat{\kappa}\rangle_D = \frac{1}{2}|\underline{u}_0|^2 n_{eff}\epsilon_{eff}^{-1}\hat{\kappa}\cdot\hat{\kappa}.$$

In the $d \to 0$ limit, the phase velocity of the plane wave in the "effective medium" is along the direction $\hat{\kappa}$ and is determined by

$$(3.4) \qquad \mathbf{v}_p = \frac{c}{n_{eff}}\hat{\kappa}.$$

Recall that we have pass bands over frequency intervals where $\epsilon_{eff}^{-1}\hat{\kappa}\cdot\hat{\kappa}$ and μ_{eff} are of the same sign. With this in mind, (3.3) and (3.4) show that in the homogenization limit the energy flow and phase velocity are in opposite directions over frequency intervals where the double negative property happens, i.e., $\epsilon_{eff}^{-1}\hat{\kappa}\cdot\hat{\kappa} < 0$ and $\mu_{eff} < 0$. These results are indicative of negative index behavior in the homogenization limit.

4. Generalized electrostatic resonances for circular coated cylinders and the Rayleigh identity. In this section we develop a Rayleigh identity for the eigenfunctions associated with generalized electrostatic resonances for coated circular cylinders. The Rayleigh method [38] has been generalized and applied to the analysis of wave propagation and the effective transport properties of composites, and the approach taken here is motivated by the recent works [22, 25, 29]. The electrostatic resonances λ_h in (2.26) are found by solving the following problem for the potential u inside a unit cell, i.e., $d = 1$:

$$(4.1) \qquad \begin{cases} \Delta u = 0 & \text{in } H, \\ \Delta u = 0 & \text{in } P, \end{cases}$$

with the boundary conditions

$$(4.2) \qquad \begin{cases} u|^- = u|^+ & \text{on } \partial P, \\ \partial_r u|_{r=a} = 0 & \text{on } \partial R, \\ \lambda[\partial_r u]_+^- = -\frac{1}{2}(\partial_r u^- + \partial_r u^+) & \text{on } \partial P, \\ u \text{ is } Y\text{-periodic.} \end{cases}$$

Consequently, in polar coordinates (r, θ), the expansions of the potential $u(r, \theta)$ are

$$(4.3) \qquad u_p(r, \theta) = \sum_{l=1}^{\infty}(A_l r^l + B_l r^{-l})\cos l\theta \qquad \text{in } P,$$

$$(4.4) \qquad u_h(r, \theta) = \sum_{l=1}^{\infty}(C_l r^l + D_l r^{-l})\cos l\theta \qquad \text{in } H.$$

From the boundary conditions (4.2), we can express A_l, C_l, and D_l in terms of B_l. Therefore we get

$$(4.5) \qquad \begin{cases} A_l = a^{-2l}B_l, \\ C_l = \left(\frac{a^{2l}b^{-2l}-2\lambda}{1-2\lambda}\right)a^{-2l}B_l, \\ D_l = \left(\frac{a^{-2l}b^{2l}-2\lambda}{1-2\lambda}\right)B_l. \end{cases}$$

The surface charge density $Q_s(\theta)$ is defined by

$$(4.6) \qquad \begin{aligned} Q_s(\theta) &= (\partial_r u_p - \partial_r u_h)|_{r=b} \\ &= 2\sum_{l=1}^{\infty}\left(\frac{b^{l-1}a^{-2l}-b^{-(l+1)}}{1-2\lambda}\right)lB_l\cos l\theta. \end{aligned}$$

The potential at an arbitrary point $G(r, \theta)$ is given by

$$(4.7) \qquad u(r, \theta) = -\frac{1}{2\pi} \sum_j \int_{\partial s_j} Q^j_{s_j}(\mathbf{t}_{(\mathbf{s_j})}) \ln(|\mathbf{r} - \mathbf{t}_{(\mathbf{s_j})}|) \mathbf{ds_j}.$$

In the summation, j refers to the jth cylinder and the vector $\mathbf{t}_{(\mathbf{s_j})}$ extended from the origin to the area element ds_j on its shell. $Q^j_{s_j}(\mathbf{t}_{(\mathbf{s_j})})$ is the surface charge density at this area element. We sum over all cylinders in the lattice and integrate over the entire surface of each cylinder. We introduce the vectors $\boldsymbol{\rho_j}$ pointing from the center of the jth cylinder to the point G and $\mathbf{s}$ pointing from the center of the jth cylinder to ∂s_j.
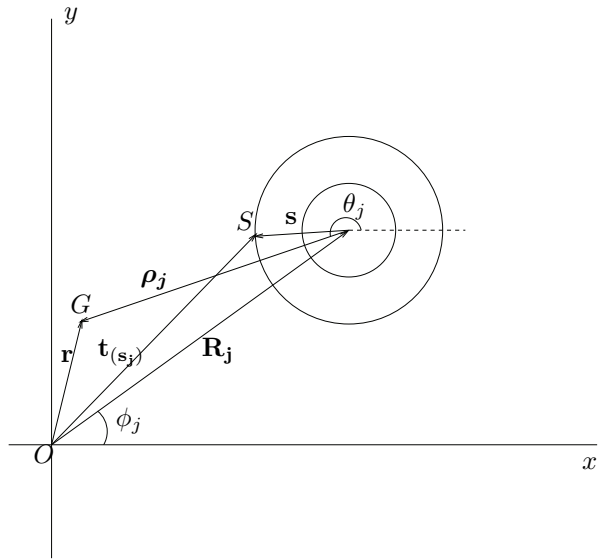

FIG. 3. *G is a typical field point, while S presents a point on the shell boundary of the jth cylinder.*

From Figure 3, it is easy to see that

$$(4.8) \qquad \mathbf{r} - \mathbf{t}_{(\mathbf{s_j})} = \boldsymbol{\rho_j} - \mathbf{s}.$$

First suppose that the field point G is in the shell of the central cylinder, i.e., $a < r < b$. Since $|\mathbf{s}| = \mathbf{b}$, $\rho_0 = \mathbf{r}$, and $|\boldsymbol{\rho_j}| > b$ for all $j \neq 0$, $a < |\mathbf{r}| < \mathbf{b}$ for $\mathbf{j} = \mathbf{0}$. Then we can expand the logarithms in (4.7):

$$\ln|\mathbf{r} - \mathbf{t}_{(\mathbf{s_j})}| = \ln|\boldsymbol{\rho_j} - \mathbf{s}|$$

$$(4.9) \qquad = \begin{cases} \ln \rho_j - \sum_{n=1}^{\infty} \frac{1}{n}(\frac{b}{\rho_i})^n \cos n(\theta' - \theta_j), & j \neq 0, \\ \ln b - \sum_{n=1}^{\infty} \frac{1}{n}(\frac{r}{b})^n \cos n(\theta' - \theta), & j = 0, \end{cases}$$

where θ' is the polar angle defining the orientation of $\mathbf{s}$ and θ_j specifies the direction of $\boldsymbol{\rho_j}$. For the jth cylinder, the surface charge density takes the form (4.6) depending on θ'. From (4.7), (4.9), and the orthonormality properties of sines and cosines, we find $(ds_j = bd\theta')$

(4.10)

$$u(r, \theta) = \sum_{l=1}^{\infty} \frac{1}{1 - 2\lambda}(a^{-2l} - b^{-2l})B_l r^l \cos l\theta + \sum_{j \neq 0} \sum_{l=1}^{\infty} \frac{1}{1 - 2\lambda}\left(\frac{a^{-2l}b^{2l} - 1}{\rho_j^l}\right) B_l \cos l\theta_j$$

for $a < r < b$.

In (4.10), the first sum is from the central cylinder and the second sum is over all the other cylinders. In the shell, we must have

$$(4.11) \qquad u(r, \theta) = u_p(r, \theta) = \sum_{l=1}^{\infty} (A_l r^l + B_l r^{-l}) \cos l\theta.$$

Plugging (4.5) and (4.10) into (4.11), we obtain the Rayleigh identity for a square array of coated cylinders:

$$(4.12) \quad \sum_{l=1}^{\infty} \left[\left(\frac{b^{-2l} - 2\lambda a^{-2l}}{1 - 2\lambda} \right) r^l + r^{-l} \right] B_l \cos l\theta = \sum_{j \neq 0} \sum_{l=1}^{\infty} \left(\frac{a^{-2l} b^{2l} - 1}{1 - 2\lambda} \right) \frac{B_l}{\rho_j^l} \cos l\theta_j$$

for $a < r < b$.

Next we suppose that the field point G is outside the shell of the central cylinder, i.e., $r > b$. The proof is similar to that for the case in the shell P. Since $r > b$, (4.9) changes to

$$(4.13) \qquad \begin{aligned} \ln |\mathbf{r} - \mathbf{t}_{(\mathbf{s_j})}| &= \ln |\boldsymbol{\rho_j} - \mathbf{s}| \\ &= \begin{cases} \ln \rho_j - \sum_{n=1}^{\infty} \frac{1}{n} (\frac{b}{\rho_i})^n \cos n(\theta' - \theta_j), & j \neq 0, \\ \ln r - \sum_{n=1}^{\infty} \frac{1}{n} (\frac{b}{r})^n \cos n(\theta' - \theta), & j = 0. \end{cases} \end{aligned}$$

Then similar to (4.10), we have
$$(4.14)$$
$$u(r, \theta) = \sum_{l=1}^{\infty} \frac{1}{1 - 2\lambda} (a^{-2l} b^{2l} - 1) B_l r^{-l} \cos l\theta + \sum_{j \neq 0} \sum_{l=1}^{\infty} \frac{1}{1 - 2\lambda} \left(\frac{a^{-2l} b^{2l} - 1}{\rho_j^l} \right) B_l \cos l\theta_j$$

for $r > b$. In the host H, we must have

$$(4.15) \qquad u(r, \theta) = u_h(r, \theta) = \sum_{l=1}^{\infty} (C_l r^l + D_l r^{-l}) \cos l\theta.$$

A calculation similar to the previous one in the shell shows that (4.12) holds for $r > b$. Therefore (4.12) is true for all $r > a$.

5. Numerical calculation of generalized electrostatic spectra for coated cylinders. Now we set $r = b$ in (4.12) and apply Rayleigh's method [38] to recover a linear system of equations to determine λ and $\{B_l\}_{l=1}^{\infty}$. Let R_j be the distance from the origin to the center of the jth cylinder and the ϕ_j be the polar angle defining the orientation of $\mathbf{R_j}$ (see Figure 3). Then for $r = b$ we have

$$(5.1) \qquad \rho_j \cos \theta_j + i\rho_j \sin \theta_j = (b \cos \theta + ib \sin \theta) - (R_j \cos \phi_j + iR_j \sin \phi_j).$$

The Rayleigh identity (4.12) with $r = b$ becomes

$$(5.2) \quad Re \sum_{l=1}^{\infty} \left[\left(\frac{b^{-2l} - 2\lambda a^{-2l}}{1 - 2\lambda} \right) B_l (b\cos\theta + ib\sin\theta)^l + B_l (b\cos\theta + ib\sin\theta)^{-l} \right]$$

$$= Re \sum_{j\neq 0} \left[\left(\frac{a^{-2}b^2 - 1}{1 - 2\lambda} \right) B_1 \left((b\cos\theta + ib\sin\theta) - (R_j\cos\phi_j + iR_j\sin\phi_j) \right)^{-1} \right.$$

$$+ \left(\frac{a^{-4}b^4 - 1}{1 - 2\lambda} \right) B_2 \left((b\cos\theta + ib\sin\theta) - (R_j\cos\phi_j + iR_j\sin\phi_j) \right)^{-2}$$

$$+ \left(\frac{a^{-8}b^8 - 1}{1 - 2\lambda} \right) B_3 \left((b\cos\theta + ib\sin\theta) - (R_j\cos\phi_j + iR_j\sin\phi_j) \right)^{-3}$$

$$+ \cdots \right].$$

Using the generalized binomial theorem on the right-hand side of (5.2), we have

$$(5.3)$$
$$Re \sum_{l=1}^{\infty} \left[\left(\frac{b^{-2l} - 2\lambda a^{-2l}}{1 - 2\lambda} \right) B_l (b\cos\theta + ib\sin\theta)^l + B_l (b\cos\theta + ib\sin\theta)^{-l} \right]$$

$$= Re \sum_{j\neq 0} \left[\left(\frac{a^{-2}b^2 - 1}{1 - 2\lambda} \right) B_1 (-1)^1 (R_j\cos\phi_j + iR_j\sin\phi_j)^{-1} \sum_{k=0}^{\infty} \left(\frac{b\cos\theta + ib\sin\theta}{R_j\cos\phi_j + iR_j\sin\phi_j} \right)^k \right.$$

$$+ \left(\frac{a^{-4}b^4 - 1}{1 - 2\lambda} \right) B_2 (-1)^2 (R_j\cos\phi_j + iR_j\sin\phi_j)^{-2} \sum_{k=0}^{\infty} \binom{1+k}{k} \left(\frac{b\cos\theta + ib\sin\theta}{R_j\cos\phi_j + iR_j\sin\phi_j} \right)^k$$

$$+ \left(\frac{a^{-8}b^8 - 1}{1 - 2\lambda} \right) B_3 (-1)^3 (R_j\cos\phi_j + iR_j\sin\phi_j)^{-3} \sum_{k=0}^{\infty} \binom{2+k}{k} \left(\frac{b\cos\theta + ib\sin\theta}{R_j\cos\phi_j + iR_j\sin\phi_j} \right)^k$$

$$+ \cdots \right].$$

Equating the coefficients of $\cos l\theta$ in (5.3) between the left- and right-hand sides, we obtain

$$(5.4) \quad \left(\frac{b^{-2l} - 2\lambda a^{-2l}}{1 - 2\lambda} \right) B_l b^l + B_l b^{-l}$$

$$= Re \left\{ \sum_{j\neq 0} \left[\left(\frac{a^{-2}b^2 - 1}{1 - 2\lambda} \right) B_1 (-1)^1 (R_j\cos\phi_j + iR_j\sin\phi_j)^{-l-1} b^l \right. \right.$$

$$+ \left(\frac{a^{-4}b^4 - 1}{1 - 2\lambda} \right) B_2 (-1)^2 (R_j\cos\phi_j + iR_j\sin\phi_j)^{-l-2} \binom{2+l-1}{l} b^l$$

$$+ \left(\frac{a^{-8}b^8 - 1}{1 - 2\lambda} \right) B_3 (-1)^3 (R_j\cos\phi_j + iR_j\sin\phi_j)^{-l-3} \binom{3+l-1}{l} b^l$$

$$\left. \left. + \cdots \right] \right\}$$

$$= \sum_{j\neq 0} \sum_{m=1}^{\infty} \left[\left(\frac{a^{-2m}b^{2m} - 1}{1 - 2\lambda} \right) \binom{m+l-1}{l} B_m (-1)^m \frac{\cos(l+m)\phi_j}{R_j^{l+m}} b^l \right]$$

$$= \sum_{m=1}^{\infty} \left[\left(\frac{a^{-2m}b^{2m} - 1}{1 - 2\lambda} \right) \binom{m+l-1}{l} B_m (-1)^m S_{l+m} b^l \right],$$

where the quantities S_n are the lattice sums

$$(5.5) \qquad S_n = \sum_{j \neq 0} \frac{\cos n\phi_j}{R_j^n}.$$

A list of numerical values for S_n is tabulated in the paper of Perrins, McKenzie, and McPhedran [29]. Rewriting (5.4) as

$$\lambda B_l = \left(\frac{b^{-2l}}{a^{-2l} + b^{-2l}} \right) B_l$$

$$(5.6) \qquad - \frac{1}{2(a^{-2l} + b^{-2l})} \sum_{m=1}^{\infty} (a^{-2m}b^{2m} - 1) \binom{m+l-1}{l} (-1)^m S_{l+m} B_m,$$

the system (5.6) may be written in the matrix form

$$(5.7) \qquad AB = \lambda B,$$

where $B = (B_1, B_2, B_3, \ldots)^T$ and the infinite dimensional matrix A has the elements

$$(5.8) \quad A_{lm} = \begin{cases} \frac{b^{-2l}}{a^{-2l}+b^{-2l}} - \frac{1}{2(a^{-2l}+b^{-2l})}(a^{-2m}b^{2m} - 1)\binom{m+l-1}{l}(-1)^m S_{l+m}, & l = m, \\ -\frac{1}{2(a^{-2l}+b^{-2l})}(a^{-2m}b^{2m} - 1)\binom{m+l-1}{l}(-1)^m S_{l+m}, & l \neq m. \end{cases}$$

TABLE 5.1
The eigenvalues corresponding to $N = 20$ with $a = 0.2$, $b = 0.4$.

λ
3.5080×10^{-1}
1.5379×10^{-2}
9.7557×10^{-4}
6.1031×10^{-5}
3.8147×10^{-6}
2.3842×10^{-7}
1.4901×10^{-8}
9.3132×10^{-10}
5.8208×10^{-10}
3.6380×10^{-10}
-1.6665×10^{-5}
-4.2856×10^{-5}
-1.1088×10^{-4}
-2.8905×10^{-4}
-7.6128×10^{-4}
-2.0285×10^{-3}
-5.5339×10^{-3}
-1.5014×10^{-2}
-4.4538×10^{-2}
-4.7947×10^{-2}

We solve (5.7) numerically, truncating the sum after N terms to find the approximation of the potential u and the generalized electrostatic resonances. Table 5.1 gives the eigenvalues corresponding to different N for $a = 0.2$ and $b = 0.4$. These numerical results confirm that the eigenvalues have an accumulation point at 0. For illustration, if λ is the first eigenvalue 3.5080×10^{-1} with $a = 0.2$ and $b = 0.4$, then we notice that $B_1 \approx 1$ and the remaining coefficients B_l's are close to 0. Hence (4.10) and (4.14)

show that the potential $u(r,\theta)$ is well approximated by

$$(5.9) \quad u(r,\theta) \approx \begin{cases} \frac{1}{1-2\lambda}(a^{-2}-b^{-2})r\cos\theta + \sum_{j\neq 0}\frac{1}{1-2\lambda}\left(\frac{a^{-2}b^2-1}{\rho_j}\right)\cos\theta_j & \text{in } P, \\ \frac{1}{1-2\lambda}(a^{-2}b^2-1)r^{-1}\cos\theta + \sum_{j\neq 0}\frac{1}{1-2\lambda}\left(\frac{a^{-2}b^2-1}{\rho_j}\right)\cos\theta_j & \text{in } H. \end{cases}$$

Equivalently (4.3) and (4.4) show that

$$(5.10) \quad u(r,\theta) \approx \begin{cases} a^{-2}r\cos\theta + r^{-1}\cos\theta & \text{in } P, \\ \left(\frac{a^2b^{-2}-2\lambda}{1-2\lambda}\right)a^{-2}r\cos\theta + \left(\frac{a^{-2}b^2-2\lambda}{1-2\lambda}\right)r^{-1}\cos\theta & \text{in } H. \end{cases}$$

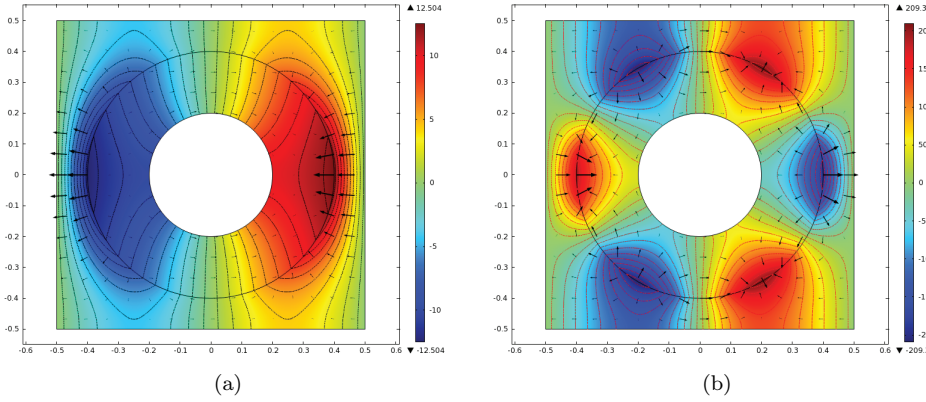The solution u corresponding to the first two eigenvalues with $a=0.2$ and $b=0.4$ are illustrated in Figure 4.

FIG. 4. (a) *the solution corresponding to the eigenvalue* $\lambda = 3.5080 \times 10^{-1}$; (b) *the solution corresponding to the eigenvalue* $\lambda = 1.5379 \times 10^{-2}$.

6. Numerical calculation of the dispersion relation and comparison with power series. In this section we verify that the leading order dispersion relation expressed in terms of effective properties is a good predictor of the dispersive behavior of the metamaterial for periods with finite size $d > 0$. The usefulness of the effective properties for predicting metamaterial behavior away from the homogenization limit can be explicitly seen from power series formula for the dispersion relation. To proceed we fix $d = c/\omega_p$ and the dimensionless ratio $\rho = d/\sqrt{\gamma}$. With this choice of variables the frequency dependent effective magnetic permeability μ_{eff} and effective dielectric permittivity ϵ_{eff} are written as

$$(6.1) \qquad \mu_{eff}\left(\frac{\omega_0}{\omega_p}\right) = \int_Y \psi_0 = \theta_H + \theta_P + \sum_{n=1}^{\infty}\frac{\mu_n\langle\phi_n\rangle_R^2}{\rho^{-2}\left(\mu_n\rho^2 - (\frac{\omega_0}{\omega_p})^2\right)}$$

and

$$\epsilon_{eff}^{-1}\left(\frac{\omega_0}{\omega_p}\right)\hat{\kappa}\cdot\hat{\kappa} = \theta_H + \frac{(\frac{\omega_0}{\omega_p})^2}{(\frac{\omega_0}{\omega_p})^2 - 1}\theta_P$$

$$(6.2) \qquad - \sum_{-\frac{1}{2}<\lambda_h<\frac{1}{2}}\left(\frac{\left((\frac{\omega_0}{\omega_p})^2-1\right)^2|\alpha_{\lambda_h}^{(1)}|^2 + 2\left((\frac{\omega_0}{\omega_p})^2-1\right)\alpha_{\lambda_h}^{(1)}\alpha_{\lambda_h}^{(2)} + |\alpha_{\lambda_h}^{(2)}|^2}{\left((\frac{\omega_0}{\omega_p})^2 - (\lambda_h+\frac{1}{2})\right)\left((\frac{\omega_0}{\omega_p})^2 - 1\right)}\right).$$

In these variables the leading order dispersion relation is given by

$$(6.3) \qquad (dk)^2 = \left(\frac{\omega_0}{\omega_p}\right)^2 n_{eff}^2,$$

where the effective index of diffraction n_{eff}^2 depends upon the direction of propagation $\hat{\kappa}$ and normalized frequency $\frac{\omega_0}{\omega_p}$ and is written as

$$(6.4) \qquad n_{eff}^2 = \mu_{eff}\left(\frac{\omega_0}{\omega_p}\right) \Big/ \left(\epsilon_{eff}^{-1}\left(\frac{\omega_0}{\omega_p}\right)\hat{\kappa}\cdot\hat{\kappa}\right).$$

The dispersion relation for the metamaterial crystal in the new variables is given by

$$(6.5) \qquad \left(\frac{\omega}{\omega_p}\right)^2 = \left(\frac{\omega_0}{\omega_p}\right)^2 + \sum_{l=1}^{\infty}(dk)^l\left(\frac{\omega_l}{\omega_p}\right)^2$$

for

$$(6.6) \qquad \{-2\pi \leq dk\hat{\kappa}_1 \leq 2\pi, -2\pi \leq dk\hat{\kappa}_2 \leq 2\pi\}.$$

It is clear from (6.5) that the roots $\frac{\omega_0}{\omega_p}$ of the effective dispersion relation (6.3) determine the leading order dispersive behavior for periods of finite size. We point out that the notion of effective properties for metamaterials has proved to be an elegant concept for explaining experimental results. Here it is seen that the power series (6.5) exhibits the precise way in which effective properties influence leading order behavior for period cells of size $d > 0$.

To verify that the leading order dispersion relation is a good predictor of the dispersive behavior of the metamaterial, we numerically compute the solutions $(\omega/\omega_p)^2$ and u^d of the nonlinear eigenvalue problem given by (2.5). These computations are carried out for different wave numbers k with propagation along the direction $(1,0)$. The simulations are carried out using COMSOL software. Here we are interested in the range $\omega/\omega_p < 1$ for which the plasmonic material has a negative permittivity, $\epsilon_P < 0$. Two examples are considered: the first example is the case of $a = 0.2d$, $b = 0.4d$, and $\epsilon_R = \gamma/d^2 = 285$, and the second example is for $a = 0.15d$, $b = 0.4d$, and $\epsilon_R = 285$. Figure 5(a)–(b) (resp., Figure 6(a)–(b)) are the graphs of the effective properties $\epsilon_{eff}^{-1}(\frac{\omega_0}{\omega_p})\hat{\kappa}\cdot\hat{\kappa}$ and $\mu_{eff}(\frac{\omega_0}{\omega_p})$, respectively. Figure 5(c) (resp., Figure 6(c)) compares the prediction given by the leading order dispersion relations $dk = \sqrt{n_{eff}^2}\frac{\omega_0}{\omega_p}$ (solid lines) with the numerical approximation of the dispersion relation given by black dots. Although the length scale of the microstructure is not infinitesimally small compared to the radiation wavelength, the numerically calculated points (black dots) fall near the solid lines predicted by the leading order dispersion relation. Notice that the magenta (lower shaded) area is the prediction of the band of double negative leading order effective properties, while the green (upper shaded) area is for the double positive band. Both graphs show that the leading order dispersion relation given by the power series can well predict the Bloch wave modes in the actual crystal up to about 20% smaller than the wavelength.

7. Conclusion. The power series method presented here provides a bottom approach to the multiscale analysis of wave propagation inside structured metallic and dielectric media. The advantage is that there are no approximations made, and the
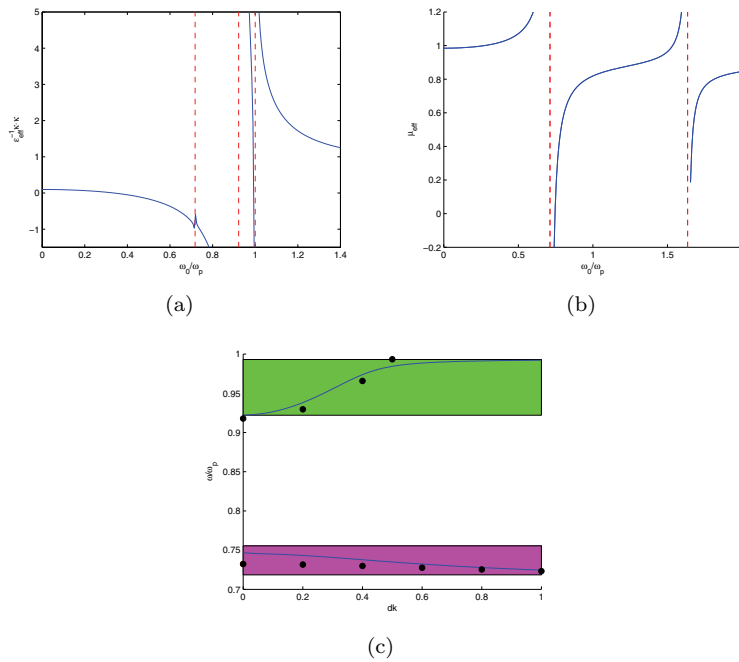
(a) (b) (c)

FIG. 5. *The case of $a = 0.2d$, $b = 0.4d$, and $\epsilon_R = 285$. Notice that the vertical dashed lines are the asymptotes.*
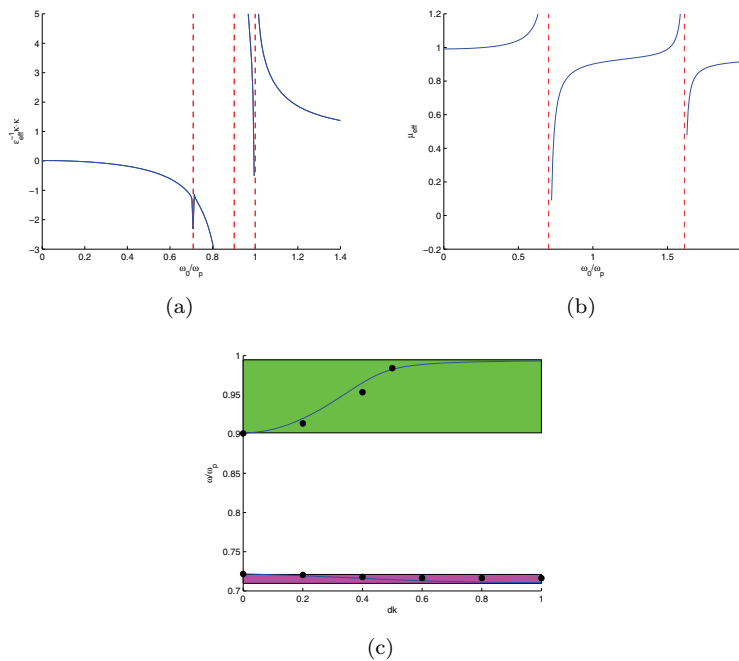

(a) (b) (c)

FIG. 6. *The case of $a = 0.15d$, $b = 0.4d$, and $\epsilon_R = 285$. Notice that the vertical dashed lines are the asymptotes.*

leading order quasi-static behavior is recovered by the leading order terms in a convergent power series solution. Formulas for frequency dependent effective properties naturally emerge from the power series solutions. The approach does not rely on dipole approximations but instead depends on the full geometric features of the structured media. Higher order terms in the series are found from simple electrostatic boundary value problems and are iteratively defined. It is seen directly from the power series that to leading order the dispersion relation is controlled by the electrostatic and Dirichlet spectra associated with the geometry of the metamaterial crystal. Direct numerical simulations for finite size period cells show that the leading order term in the power series for the dispersion relation is a good predictor of the dispersive behavior of the metamaterial. Collectively these features open up the opportunity for computational design of microstructure for the manipulation of spectral properties through control of electrostatic and Dirichlet spectra.

REFERENCES

[1] A. ALU, *First principles homogenization theory for periodic metamaterial arrays*, Phys. Rev. B, 84 (2011), 075153.

[2] A. ALU AND N. ENGHETA, *Dynamical theory of artificial optical magnetism produced by rings of plasmonic nanoparticles*, Phys. Rev. B, 78 (2008), 085112.

[3] N. O. BABYCH, I. V. KAMOTSKI, AND V. P. SMYSHLYAEV, *Homogenization of spectral problems in bounded domains with doubly high contrast*, Netw. Heterog. Media, 3 (2008), pp. 413–436.

[4] D. J. BERGMAN, *The dielectric constant of a simple cubic array of identical spheres*, J. Phys. C Solid State Phys., 12 (1979), pp. 4947–4960.

[5] C. F. BOHREN AND D. H. HUFFMAN, *Absorption and Scattering of Light by Small Particles*, Wiley, Weinheim, 2004.

[6] G. BOUCHITTÉ AND C. BOUREL, *Homogenization of finite metallic fibers and 3D-effective permittivity tensor*, Commun. Comput. Phys., to appear.

[7] G. BOUCHITTÉ AND D. FELBACQ, *Homogenization near resonances and artificial magnetism from dielectrics*, C. R. Math. Acad. Sci. Paris, 339 (2004), pp. 377–382.

[8] G. BOUCHITTÉ AND D. FELBACQ, *Negative refraction in periodic and random photonic crystals*, New J. Phys., 7 (2005), 159.

[9] G. BOUCHITTÉ AND B. SCHWEIZER, *Homogenization of Maxwell's equations in a split ring geometry*, Multiscale Model. Simul., 8 (2010), pp. 717–750.

[10] O. P. BRUNO, *The effective conductivity of strongly heterogeneous composites*, Proc. Roy. Soc. London Ser. A, 433 (1991), pp. 353–381.

[11] Y. CHEN AND R. LIPTON, *Tunable double negative band structure from non-magnetic coated rods*, New J. Phys., 12 (2010), 083010.

[12] Y. CHEN AND R. LIPTON, *Resonance and double negative behavior in metamaterials*, Arch. Ration. Mech. Anal., to appear.

[13] R. L. CHERN AND D. FELBACQ, *Artificial magnetism and anticrossing interaction in photonic crystals and split-ring structures*, Phys. Rev. B, 79 (2009), 075118.

[14] G. DOLLING, C. ENRICH, M. WEGENER, C. M. SOUKOULIS, AND S. LINDEN, *Low-loss negative-index metamaterial at telecommunication wavelengths*, Opt. Lett., 31 (2006), pp. 1800–1802.

[15] D. FELBACQ AND G. BOUCHITTÉ, *Homogenization of wire mesh photonic crystals embedded in a medium with a negative permeability*, Phys. Rev. Lett., 94 (2005), 183902.

[16] S. P. FORTES, R. P. LIPTON, AND S. P. SHIPMAN, *Sub-wavelength plasmonic crystals: Dispersion relations and effective properties*, Proc. R. Soc. Lond. Ser. A Math. Phys. Eng. Sci., 466 (2010), pp. 1993–2020.

[17] S. P. FORTES, R. P. LIPTON, AND S. P. SHIPMAN, *Convergent power series for fields in positive or negative high-contrast periodic media*, Comm. Partial Differential Equations, 36 (2011), pp. 1016–1043.

[18] K. C. HUANG, M. L. POVINELLI, AND J. D. JOANNOPOULOS, *Negative effective permeability in polaritonic photonic crystals*, Appl. Phys. Lett., 85 (2004), pp. 543–545.

[19] J. HUANGFU, L. RAN, H. CHEN, X. ZHANG, K. CHEN, T. M. GRZEGORCZYK, AND J. A. KONG, *Experimental confirmation of negative refractive index of a metamaterial composed of Ω-*

like metallic patterns, Appl. Phys. Lett., 84 (2004), pp. 1537–1539.

[20] R. V. KOHN AND S. P. SHIPMAN, *Magnetism and homogenization of microresonators*, Multi-scale Model. Simul., 7 (2008), pp. 62–92.

[21] R. C. MCPHEDRAN AND G. W. MILTON, *Bounds and exact theories for the transport properties of inhomogeneous media*, Appl. Phys. A, 26 (1981), pp. 207–220.

[22] R. C. MCPHEDRAN, N. A. NICOROVICI, L. C. BOTTEN, AND A. B. MOVCHAN, *Advances in the Rayleigh multipole method for problems in photonics and phononics*, in IUTAM Symposium on Mechanical and Electromagnetic Waves in Structured Media, R. C. McPhedran, L. C. Botten, and N. A. Nicorovici, eds., Kluwer Academic Publishers, Dordrecht, The Netherlands, 2001, pp. 15–28.

[23] G. W. MILTON, *The Theory of Composites*, Cambridge University Press, Cambridge, UK, 2002.

[24] G. W. MILTON, *Realizability of metamaterials with prescribed electric permittivity and magnetic permeability tensors*, New J. Phys., 12 (2010), 033035.

[25] N. A. NICOROVICI, R. C. MCPHEDRAN, AND G. W. MILTON, *Transport properties of a 3 phase composite material: The square array of coated cylinders*, Proc. R. Soc. Lond. Ser. A, 422 (1993), pp. 599–620.

[26] J. PENDRY, A. HOLDEN, D. ROBBINS, AND W. STEWART, *Low frequency plasmons in thin-wire structures*, J. Phys.: Condens. Matter, 10 (1998), pp. 4785–4809.

[27] J. PENDRY, A. HOLDEN, D. ROBBINS, AND W. STEWART, *Magnetism from conductors and enhanced nonlinear phenomena*, IEEE Trans. Microw. Theory Tech., 47 (1999), pp. 2075–2084.

[28] L. PENG, L. RAN, H. CHEN, H. ZHANG, L. A. KONG, AND T. M. GRZEGORCZYK, *Experimental observation of left-handed behavior in an array of standard dielectric resonators*, Phys. Rev. Lett., 98 (2007), 157403.

[29] W. T. PERRINS, D. R. MCKENZIE, AND R. C. MCPHEDRAN, *Transport properties of regular arrays of cylinders*, Proc. Roy. Soc. London Ser. A, 369 (1979), pp. 207–225.

[30] R. F. SERVICE, *Next wave of metamaterials hopes to fuel the revolution*, Science, 327 (2010), pp. 138–139.

[31] V. SHALAEV, *Optical negative-index metamaterials*, Nat. Photon., 1 (2007), pp. 41–48.

[32] V. M. SHALAEV, W. CAI, U. K. CHETTIAR, H. K. YUAN, A. K. SARYCHEV, V. P. DRACHEV, AND A. V. KILDISHEV, *Negative index of refraction in optical metamaterials*, Opt. Lett., 30 (2005), pp. 3356–3358.

[33] R. A. SHELBY, D. R. SMITH, AND S. SCHULTZ, *Experimental verification of a negative index of refraction*, Science, 292 (2001), pp. 77–79.

[34] S. SHIPMAN, *Power series for waves in micro-resonator arrays*, in Proceedings of the 13th International IEEE Conference on Mathematical Methods in Electrodynamic Theory, Kyiv, Ukraine, 2010.

[35] G. SHVETS AND Y. URZHUMOV, *Engineering the electromagnetic properties of periodic nano-structures using electrostatic resonances*, Phys. Rev. Lett., 93 (2004), 243902.

[36] D. R. SMITH, W. PADILLA, D. VIER, S. NEMAT-NASSER, AND S. SCHULTZ, *Composite medium with simultaneously negative permeability and permittivity*, Phys. Rev. Lett., 84 (2000), pp. 4184–4187.

[37] D. R. SMITH AND J. B. PENDRY, *Homogenization of metamaterials by field averaging*, J. Opt. Soc. Amer. B, 23 (2006), pp. 391–403.

[38] J. W. STRUTT, *On the influence of obstacles arranged in rectangular order upon the properties of a medium*, Phil. Mag., 34 (1892), pp. 481–502.

[39] V. G. VESELAGO, *The electrodynamics of substances with simultaneously negative values of ϵ and μ*, Soviet Phys. Uspekhi, 10 (1968), pp. 509–514.

[40] K. VYNCK, D. FELBACQ, E. CENTENO, A. I. CABUZ, D. CASSAGNE, AND B. GUIZAL, *All-dielectric rod-type metamaterials at optical frequencies*, Phys. Rev. Lett., 102 (2009), 133901.

[41] M. S. WHEELER, J. S. AITCHISON, AND M. MOJAHEDI, *Coated non-magnetic spheres with a negative index of refraction at infrared frequencies*, Phys. Rev. B, 73 (2006), 045105.

[42] V. YANNOPAPAS, *Negative refractive index in the near-UV from Au-coated CuCl nanoparticle superlattices*, Phys. Stat. Sol. (RRL), 1 (2007), pp. 208–210.

[43] V. YANNOPAPAS, *Artificial magnetism and negative refractive index in three-dimensional meta-materials of spherical particles at near-infrared and visible frequencies*, Appl. Phys. A, 87 (2007), pp. 259–264.

[44] F. ZHANG, S. POTET, J. CARBONELL, E. LHEURETTE, O. VANBESIEN, X. ZHAO, AND D. LIPPENS, *Negative-zero-positive refractive index in a prism-like omega-type metamaterial*, IEEE Trans. Microw. Theory Tech., 56 (2008), pp. 2566–2573.

[45] S. ZHANG, W. FAN, B. K. MINHAS, A. FRAUENGLASS, K. J. MALLOY, AND S. R. J. BRUECK,

Midinfrared resonant magnetic nanostructures exhibiting a negative permeability, Phys. Rev. Lett., 94 (2005), 037402.

[46] V. V. ZHIKOV, *On an extension of the method of two-scale convergence and its applications*, Sb. Math., 191 (2000), pp. 973–1014.

[47] V. V. ZHIKOV, *On spectrum gaps of some divergent elliptic operators with periodic coefficients*, St. Petersburg Math. J., 16 (2004), pp. 1–18.

[48] X. ZHOU AND X. P. ZHAO, *Resonant condition of unitary dendritic structure with overlapping negative permittivity and permeability*, Appl. Phys. Lett., 91 (2007), 181908.